Food Chemistry: X 22 (2024) 101452

Contents lists available at ScienceDirect

Food Chemistry: X

journal homepage: www.sciencedirect.com/journal/food-chemistry-x

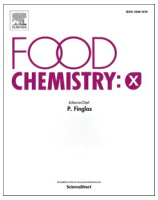

Protein of yak milk residue: Structure, functionality, and the effects on the quality of non-fat yogurt

Guangfan Qu [a,1], Feiyan Yang [a,1], Hanzhi Zhang [a], Yanfeng Liu [a], Xudong He [a], Fei Liu [a], Shuguo Sun [a,*], Zhang Luo [b,*]

[a] National Engineering Laboratory for Deep Process of Rice and Byproducts, Hunan Key Laboratory of Grain-oil Deep Process and Quality Control, Hunan Key Laboratory of Forestry Edible Resources Safety and Processing, College of Food Science and Engineering, Central South University of Forestry and Technology, Changsha 410004, Hunan, China

[b] College of Food Science, Tibet Agriculture & Animal Husbandry University, Nyingchi 860000, Tibet, China

ARTICLE INFO

Keywords:
Protein
Structure
Functionality
Non-fat yogurt
Sensory

ABSTRACT

The purpose of this study was to compare the structural and functional of protein from yak milk residue, which collected from different elevations (MRP1 and MRP2) in Tibet, as well as their potential for enhancing the quality of non-fat yogurt. The results showed that MRP1 exhibited higher levels of β-sheet, turbidity, particle size, and gel properties. MRP2 had better flexibility, emulsification, foaming, water/oil absorption capacity. The addition of MRP1 (3%) could improve texture and sensory properties of yogurt. Although MRP2 yogurt had higher hardness, gumminess, chewiness and water holding capacity, poor mouthfeel. Rheological test showed that MRPs yogurt exhibited typical gel-like and shear-thinning behavior. Moreover, the fortification of non-fat yogurts with MRP1 brought the formation of larger protein clusters with a more tightly knit network of smaller pores. These results indicate that MRP1 can be used as a fat substitute to improve the quality of non-fat yogurt.

Introduction

Yak milk residue is obtained through natural fermentation, filtration, and drying after heating fresh or skimmed yak milk (at 50 ~ 60 °C) following the extraction of ghee (Yang et al., 2021c). The milk residue is a hard, slag-like substance that appears white in color and has a sour taste. It is also rich in protein, amino acids, minerals, lactose and vitamins (Yang et al., 2021a). The consumption of this protein-rich food source is crucial for plateau herders because it can enhance their immune system, facilitate intestinal digestion, and nourish vital energy and blood (Qin et al., 2021). Consequently, it aids Tibetan people withstand cold temperature and adapting to low oxygen environments on the plateau (Yang et al., 2021a). Currently, the research and development of yak milk residue is relatively simplistic, primarily focusing on feed processing, resulting in limited utilization value.

The primary component of yak milk residue is protein, with Tibetan milk residue containing up to 70 % protein (Yang et al., 2021c). This protein exhibits comparable biological activity to other proteins. Yang et al. (2021a) and Qin et al. (2021) discovered that proteolytic peptides derived from yak milk residue mitigate H_2O_2-induced apoptosis by modulate the expression of antioxidant Nrf2 and its target genes Keap1, Nrf2, HO-1, and NQO1, thereby alleviate H_2O_2-induced oxidative stress in human vein endothelial cells. In addition, previous studies have identified casein (αs1-CN, αs2-CN, β-CN, and κ-CN) as the predominant proteins in yak milk residue, accompanied by a minor presence of whey protein (Yang et al., 2021a). Casein exhibits various functional properties, including emulsification, foaming, water and oil absorption, gelation, and plays a crucial role in food sensory perception and flavor (Chen et al., 2022). However, its characteristics are influenced by the source of raw materials as well as extraction and modification methods (Yang et al., 2021c). The structure, functional properties, and differences in food applications of yak milk proteins from plateau areas remain limited. Therefore, it is imperative to conduct a comprehensive study on the characteristics of yak milk residue isolate protein.

In recent years, yogurt has emerged as one of the most popular fermented dairy products among consumers due to its unique flavor and

* Corresponding authors at: College of Food Science and Engineering, Central South University of Forestry and Technology, No. 498, Shaoshan Road, Changsha 410004, Hunan, PR China (S. Sun). College of Food Science, Tibet Agriculture & Animal Husbandry University, No. 100, Yucai West Road, Bayi District, Nyingchi 860000, Tibet, China (Z. Luo).

E-mail addresses: sshuguo@163.com (S. Sun), Luozhang1759@sohu.com (Z. Luo).

[1] These authors contributed equally to this work.

https://doi.org/10.1016/j.fochx.2024.101452
Received 22 February 2024; Received in revised form 23 April 2024; Accepted 5 May 2024
Available online 16 May 2024

taste resulting from fermentation by lactic acid bacteria (Hashim et al., 2021). Furthermore, it offers various health benefits including alleviating diarrhea, reducing serum cholesterol levels, promoting a balanced intestinal microflora, and preventing lactose intolerance (Gantumur et al., 2023). Due to concerns over excessive fat intake and its associated health risks, such as obesity and cardiovascular diseases, an increasing number of consumers are opting for low-fat/non-fat yoghurts (Atallah et al., 2020). The limited fat content, low viscosity, weak gelation, and whey precipitation in low-fat/non-fat yogurt significantly reduced its shelf life (Gantumur et al., 2023). Several studies have demonstrated that incorporating whey protein (Atallah et al., 2020), starch (Lee and Kang, 2024), and konjac glucomannan (Dai et al., 2016) as fat substitutes can enhance the viscosity, texture, and sensory attributes of low-fat yogurt. The global population is experiencing rapid growth, which is accompanied by a gradual increase in consumer demand. Therefore, the development of novel fat substitutes has become particularly crucial to meet these evolving consumer needs. However, there is currently no existing literature on the utilization of yak milk residue protein as a fat substitute in skim yogurt.

Therefore, the objective of this study is to analyze the structural and functional characteristics of protein from yak milk residue in Linzhi (2968 m above sea level) and Jiali (4700 m above sea level) regions of Tibet, respectively. Additionally, we also investigate the impact of incorporating yak milk residue protein on sensory attributes, texture, rheology, and microstructure of skim yogurt, compared with commercial whey protein concentrates (WPC).

2. Materials and methods

2.1. Materials

This study collected a total of 12 fresh yak milk residue samples, which were divided into two groups of 6 each. The samples were obtained from two distinct elevations in Tibet, China, and the collection period spanned from September to December 2021. The samples are numbered as MRP1 [31.54 N, 92.55E, 4,700 m above mean sea level (Jiali)] and MRP2 [29.61 N, 94.36E, 2,968 m above mean sea level (Nyingchi)]. Six samples of yak milk residue were obtained from six different farmers' markets at the same elevation, and then the yak milk residue samples are mixed to reduce the experimental error caused by improper sampling. All samples were immediately transported to the laboratory and stored at 4 °C.

Sodium dodecyl sulfate polyacrylamide gel electrophoresis (SDS-PAGE) gel preparation kit, marker (10–170 kDa) and bovine serum protein were purchased from Beijing Suolaibao Biotechnology Co. Ltd. (Beijing, China). Whey protein powder was purchased from New Zealand Fonterra Trading (Shanghai) Co. Ltd. (Shanghai, China). Commercial yogurt starter is purchased from Beijing Chuanxiu International Trade Co. Ltd. (Beijiang, China) and contains Lactobacillus bulgaricus, Streptococcus thermophilus, Lactobacillus acidophilus, Lactobacillus plantarum and Lactobacillus casei. All other analytical grade chemicals were purchased from Sinopharm Chemical Reagents Co. Ltd. (Shanghai, China). Other reagents are analytical grade and purchased from Sinopharm Chemical Reagents Co. Ltd. (Shanghai, China).

2.2. Preparation of yak milk residue proteins (MRPs)

The residue of yak milk was crushed and then passed through a 200-μm sieve. The powder was immediately degreased with petroleum ether at a ratio of 1:10 (w/v), maintained at 25 °C for 4 h, and repeated 3 times. Subsequently, the defatted yak milk residue powder was obtained through drying. The MRP preparation was referenced to the method of (Ding et al., 2022). Specifically, defatted yak milk residue powder was dissolved in deionized water at a ratio of 1:10 (w/v). The pH of the yak milk residue powder solution was adjusted to 9.0 using a 2 mol/L NaOH solution and stirred at 25 °C for 6 h. After centrifugation at 10,000 g for 15 min at 4 °C, the supernatant was collected and adjusted to a pH of 4.0 using 2 mol/L HCl. After being incubated for 40 min, the solution was subjected to centrifugation at 10,000 g and 4 °C for 15 min to obtain MRP precipitation. The MRP precipitate was dissolved in deionized water at a ratio of 1: 5 (w/v), and the pH value of the obtained solution was adjusted to 7 with 1 mol/L NaOH solution, and then dialysis continued for 24 h. Finally, MRP was obtained by freeze drying.

2.3. Structural properties of MRPs

2.3.1. Sodium dodecyl sulfate–polyacrylamide gel electrophoresis (SDS-PAGE)

SDS-PAGE of MRPs was performed with 8 % separation gel and 5 % concentrated gel. Mix the protein solution (1 mg/mL) with sample buffer (containing 60 mmol/L Tris-HCl, 25 % glycerol, 1 mg/mL bromophenol blue, 14.4 mmol/L SDS, and 0.1 % mercaptoethanol) in a ratio of 4:1. Thoroughly shake and mix the solution before immersing it in a boiling water bath for 5 min. Subsequently, allow it to cool to room temperature before sampling 7 μL per well. Electrophoresis was performed at 60 V for 60 min, and then at 120 V for 120 min. The gel was dyed with coomassie brilliant blue (R-250) overnight, and then the gel was decolorized with decolorizing solution (absolute ethanol: acetic acid: water = 1:1:8, v/v/v). Imaging was performed using a gel imaging system (ChemiDocTM XRS^{+}, Bio-Rad Laboratories, USA) (Ma et al., 2018).

2.3.2. Fourier transform infrared spectroscopy (FTIR)

The infrared spectra of the MRPs were measured using an FTIR spectrometer (Vertex 70, Bruker Co., Karlsruhe, Germany) at wavelengths of 400–4000 cm^{-1} according to the method of Dang et al. (2023). The secondary structure of MRPs in the I band of the spectral amide region was analyzed using PeakFit V4.12 software.

2.3.3. Intrinsic fluorescence spectroscopy

The intrinsic fluorescence spectroscopy of the MRPs were measured using a fluorescence spectrophotometer (G9800A, Agilent Technologies Inc., California, USA) according to the method of Ma et al. (2018). The excitation wavelength is 280 nm, the emission wavelength ranges from 300 to 500 nm, and the excitation and emission slits are both 10 nm.

2.3.4. Flexibility of MRPs

Flexibility was determined by referring to the method described by Li et al. (2019). Combine 1 mg/mL MRPs solution with 1 mg/mL trypsin solution (containing Tris-HCl buffer at a concentration of 0.05 mol/L and pH 8.0) in a volumetric ratio of 16:1 (v/v). The hydrolysis was subsequently performed at 38 °C for 5 min, followed by the addition of an equal volume of trichloroacetic acid (5 %) to terminate the enzymatic reaction with the above solution. Centrifuge the mixture at 4000g for 30 min to collect the protein supernatant, and measure its absorbance at a wavelength of 280 nm.

2.3.5. Surface hydrophobicity (H_0)

H_0 of MRPs was determined using ANS fluorescent probe. A protein solution with a concentration of 0.05 ~ 0.5 mg/mL was prepared by diluting MRPs with a 0.01 mol/L phosphate buffer (pH7.0). Protein solutions with different concentrations (4 mL each) were individually mixed with 20 μL of ANS (8 mmol/L). The fluorescence intensity of the resulting mixture was measured using a fluorescence spectrophotometer (F4600, Shimadzu Co., Kyoto, Japan) at excitation wavelength of 390 nm and emission wavelength of 470 nm (Dang et al., 2023).

2.3.6. Particle size and zeta potential

The Particle size and zeta potential of the MRPs were measured using a Nanometer particle size analyzer (Nano ZS, Malvern In-struments Ltd, Worcestershire, UK) according to the method of Li et al., (2021).

2.3.7. Turbidity measurement

MRPs was diluted with 5 mmol/LPBS (pH 7) to obtain 1 mg/mL protein solution. The absorbance of protein solution at 340 nm was measured by ultraviolet spectrophotometer (UV-2600, Shimadzu Co., Kyoto, Japan). The absorbance is protein turbidity (Jia et al., 2015).

2.3.8. Gelation properties

For gel properties, prepare 20 % (w/v) protein isolate suspensions with distilled water and heat in a 70 °C water bath for 60 min. Immediately cool and place overnight in a 4 °C refrigerator. The gel sample was centrifuged at a speed of 8000 g/min for 15 min, and the weight of the gel before and after centrifugation was recorded (Sun et al., 2023). The WHC calculation of MRPs was as follows:

$$WHC(\%) = \frac{W_2}{W_1} \times 100$$

where W_1 and W_2 represent the weight (g) of the gel before and after centrifugation.

2.4. Functional properties of MRPs

2.4.1. Protein solubility (PS)

The PS of MRPs was determined according to Bradford method reported by Sun et al. (2023). The protein sample was diluted with deionized water to obtain 1 mg/mL protein solution, which was centrifuged at 10,000 g/min for 20 min, and the absorbance value of supernatant at 595 nm was recorded. The content of soluble protein in supernatant was calculated by standard curve of bovine serum albumin (BSA). PS is the ratio of protein content of supernatant to total protein content.

2.4.2. Water absorption capacity (WAC) and oil absorption capacity (OAC)

Take 0.4 g protein sample and mixed it with 10 mL deionized water/soybean oil, swirl evenly, and centrifuge at 8000 g/min for 15 min. Pour out the supernatant and weigh the precipitate. WAC/OAC is expressed as the weight of water/oil adsorbed per gram of MRPs (Ma et al., 2018).

2.4.3. Emulsifying properties

The EAI and ESI of MRPs were measured following the method of Dang et al. (2023). Briefly, 1 mg/mL protein solution was mixed with soybean oil at a ratio of 3:1 and homogenized at 10000 rpm for 2 min. 50 μL of emulsion was mixed with 5 mL of 0.1 %SDS solution, and the absorbance of the mixed solution at 500 nm was determined with 0.1 % SDS as control. The EAI and ESI values were calculated as follows:

$$EAI(m^2/g) = \frac{2 \times 2.302 \times A_0 \times N}{C \times 0.25 \times 10^4}$$

$$ESI(min) = 10 \times \frac{A_0}{A_0 - A_{10}}$$

where N is the dilution multiple; C is the protein concentration (mg/mL); A_0 and A_{10} are absorbance at 0 min and 10 min, respectively.

2.4.4. Foaming capacity (FC) and foam stability (FS)

The FC and FS values were measured using the method described by Sun *et al.*

(2023) with slight modifications. Briefly, 1.2 g protein was dissolved in 20 mL deionized water and homogenized at 10000 rpm for 2 min. The foam volumes after homogenization and standing for 30 min were recorded respectively. The FC and FS values were calculated as follows:

$$FC(\%) = \frac{V_1}{V_0} \times 100$$

$$FS(\%) = \frac{V_2}{V_0} \times 100$$

where V_0 is the volume of the solution; V_1 and V_2 are respectively the foam volume (mL) after homogenization and the foam volume (mL) after standing for 30 min.

2.5. Preparation of fortified yogurt

Ten varieties of yogurt were prepared using skim milk with a protein content of 3.5 %, no fat, and a carbohydrate content of 5.0 %. Glass containers filled with skim yogurt were supplemented with 1.5 %, 3 %, and 4.5 % WPC, MRP1 and MRP2, respectively. All samples were subjected to stirring in a water bath at 45 °C for 30 min to ensure complete dissolution of WPC, MRP1, and MRP2. Subsequently, homogenization was performed at a speed of 10000 rpm for 2 min followed by pasteurization at a temperature of 95 °C for 15 min. The samples were rapidly cooled to approximately 40 °C before inoculating them with commercial yogurt starter at a concentration of 1 g/L. Fermentation was carried out at a temperature of 42 °C until the pH reached around pH4.4, after which fermentation was halted. The resulting yogurt samples were stored in refrigeration conditions at a temperature of 4 °C for 24 h before being kept continuously under the same conditions for 14 d. The samples were collected during each storage time point for further analysis.

2.6. Characteristics of fortified yogurt

2.6.1. Sensory evaluation

This study protocol and consent procedure received ethical approval from the Research Ethics Committee of Central South University of Forestry and Technology. In addition, all sensory team members provided written informed consent.

The sensory evaluation of yogurt was used the method described by Lee et al. (2021) with slight modifications. Ten students majoring in food science from Central South University of Forestry and Technology were invited to conduct random sensory evaluations. They were well trained in basic sensory evaluation skills. Team members evaluated 10 kinds of yogurt in a separate room. The evaluation criteria of yogurt included color (20 points), flavor (20 points), mouthfeel (20 points), taste (20 points), solidification (20 points), overall acceptability (10 points).

2.6.2. Whiteness (W_H), water holding capacity (WHC) and titratable acidity (TA)

The L*, a* and b* values of yogurt were determined by Hunter LabScan colorimeter (UltraScan Pro 1166, USA). The whiteness of yogurt is calculated according to the following formula:

$$W_H = 100 - [(100 - L^*)^2 + (a^*)^2 + (b^*)^2]^{1/2}$$

The determination of water-holding capacity of yogurt refers to the method described by Yang et al. (2021b). The content of TA in yogurt is determined according to China national food safety standard-food acidity (GB 5009.239–2016).

2.6.3. Texture determination

Texture analyzer (TA, Taxtplus, stable micrio system, UK) was used to determine the texture parameters of yogurt, including hardness, adhesiveness, gumminess and chewiness. Measurement parameters: the pre-measurement speed, the mid-measurement speed and the post-measurement speed are 3 mm/s, 1 mm/s and 3 mm/s respectively, the trigger force is 5 g, the strain force is 35 %, and the sample compression interval is 5 s (Yang et al., 2021b).

2.6.4. Rheological property

The static and dynamic rheological properties of yogurt were

determined by rheometer (DHR-2, Rheotest Company, Germany) equipped with parallel plate geometric sensor (diameter 35.00 mm, gap 1 mm). In short, the shear rate range was 0.1 s^{-1} to 100 s^{-1} at 25 °C. After the shear rate program was finished, the frequency scanning test with the frequency range of 0.1–10 Hz was carried out under the condition of constant strain of 0.1 % and 25 °C. During the test, the viscosity, shear stress, storage modulus (G′) and loss modulus (G″), were monitored (Ban et al., 2020).

2.6.5. Microstructural analysis

The changes of microstructure of yogurt in different storage time were observed by laser confocal scanning microscope (DMI3000B, Leica Corporation, Wetzlar Germany). Slices of yogurt were cut on the glass slide with a surgical knife, stained with 30 μL rhodamine B (1 mg/mL), and covered with a cover glass. After the slide was left in the dark for 15 min, CLSM observation was performed (excitation wavelength 555 nm, emission wavelength 580 nm).

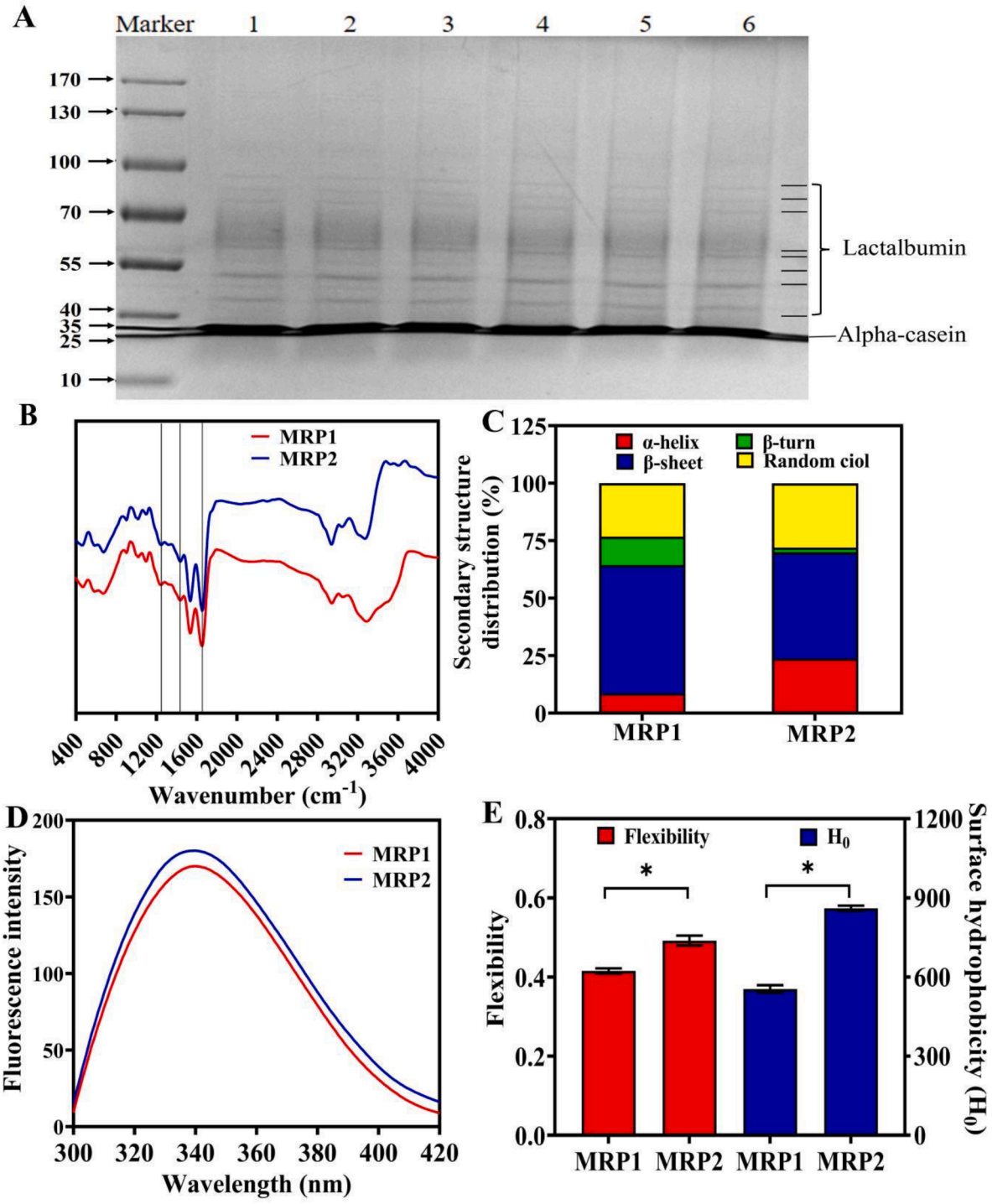

Fig. 1. (A) SDS-PAGE of MRP1(Lanes 1–3) and MRP2(Lanes 4–6). (B) FTIR spectra of MRPs. (C) Relative content of secondary structure of MRPs. (D) Intrinsic fluorescence spectra of MRPs. (E) Flexibility and surface hydrophobicity of MRPs. Symbol * show the statistical difference at $p < 0.05$.

2.7. Statistical analysis

All experiments were repeated three times, and the data were expressed as mean with standard deviations. Statistical analysis was conducted using SPSS 22.0 (SPSS Co., Ltd., Chicago, IL, USA). Significant differences were analyzed by Duncan's multiple range test at $p < 0.05$. All figures were performed using GraphPad Prism 8 (GraphPad Lab Corp., Northampton, MA, USA).

3. Results and discussion

3.1. SDS-PAGE of MRPs

The arrangement of protein subunits is intricately linked to their functions and gel properties (Sun et al., 2023). Therefore, SDS-PAGE was employed to analyze the molecular weight of protein subunits in yak milk residue. MRP1 (Lane 1–3) and MRP2 (Lane 4–6) show the identical characteristic bands (Fig. 1A), displaying distinct α and β subunit bands, with the intensity and breadth of these bands reflecting the abundance of each respective subunit. The noteworthy point is that MRP1 and MRP2 are primarily composed of casein (β-casein, α-S1-casein, and α-S2-casein) as well as whey proteins (β-lactoglobulin and serum albumin) (Yang et al., 2021a). Additionally, our previous research has also shown that MRP2 contains more β-lactoglobulin while MRP1 has a higher level of serum albumin (Yang et al., 2021a). Therefore, the yogurt containing MRP2 protein demonstrates increased hardness compared to that containing MRP1, while the latter exhibits superior viscoelasticity (Table 1), ascribed to its lower β-lactoglobulin content and higher serum albumin content. The observed phenomenon may be attributed to the fact that β-lactoglobulin gel can undergo disulfide bonding and electrostatic interactions during the yogurt preparation process, resulting in the formation of a stable three-dimensional network structure (Anema, 2021). In contrast, serum albumin gel formation is solely reliant on hydrogen bonding (Anema, 2021). In addition, the reduced or absent presence of β-lactoglobulin is a crucial factor determining the high WHC of MRP1. This leads to well-structured and whey-free precipitation in MRP1 protein-based yogurt (Fig. 4C). Therefore, the yogurt containing MRP2 protein demonstrates increased hardness compared to that containing MRP1, while the latter exhibits superior viscoelasticity (Table 1), ascribed to the lower β-lactoglobulin content and higher serum albumin content in MRP1. The observed phenomenon may be attributed to the fact that during the yogurt preparation process, β-lactoglobulin gel can undergo disulfide bond and electrostatic interactions, leading to the formation of a stable three-dimensional network structure (Silva et al., 2018). In contrast, serum albumin gel formation is solely reliant on hydrogen bonding (Silva et al., 2018). In conclusion, yaks living at different altitudes affect the protein structure of its milk dregs, which eventually leads to different functional properties.

3.2. FTIR spectrum analysis of MRPs

FTIR spectroscopy is employed for the analysis of protein secondary structure. The infrared spectra of MRP1 and MRP2 exhibit distinct characteristic absorption peaks within the amide I region, amide II and amide III (Fig. 1B). Amide I (1700–1600 cm^{-1}) is the pivotal absorption feature within the protein FT-IR spectrum, which is intimately associated with the secondary structure of protein (Sun et al., 2023). The relative content of secondary structure in MRPs was determined by fitting the curve and calculating the area under the amide 1 region, as depicted in Fig. 1C. MRP1 exhibits an α-helix content of 8.63 %, while MRP2 demonstrates a higher α-helix content at 23.79 %. In contrast, MRP1 displays a β-sheet content of 55.74 % compared to MRP2 slightly lower value of 46.16 %. Moreover, MRP1 possesses a β-turn content of 12.37 %, whereas this proportion is significantly lower at only 2.06 % for MRP2. The random coil conformation constitutes approximately 23.26 % in MRP1 and slightly more at 27.99 % in its counterpart, namely MRP2. These findings suggest that both proteins predominantly adopt β-sheet structures. Intriguingly, there appears to be a relatively higher abundance of α-helices and random coils present in MRP2 when compared to its counterpart, namely MRP1. The observed outcomes may be attributed to the genetic characteristics of yaks in diverse growth environments. The study conducted by Yang and his colleague revealed significant regional variations in the protein composition of yak milk (Yang et al., 2021c). The relative content of different secondary structures is related to the texture characteristics of protein gel (Dang et al., 2023). The presence of a higher β-sheet content in MRP1 contributes to enhanced viscoelasticity, resulting in reduced yogurt hardness. Conversely, MRP2 with a lower β-sheet content exhibits increased hardness. Dang and his group found that soybeans with higher β-sheet content have lower tofu hardness (Dang et al., 2023). However, other studies show a positive correlation between the β-sheet content and the hardness of various gel systems (Zheng et al., 2021). This variation may

Table 1
Texture parameters during the storage process of skim yogurt with different concentrations of WPC, MRP1, and MRP2.

Yogurt	Hardness (g)			Adhesiveness (g.*sec*)			Gumminess (g)			Chewiness (g)		
	0 (d)	7 (d)	14 (d)	0 (d)	7 (d)	14 (d)	0 (d)	7 (d)	14(d)	0 (d)	7 (d)	14 (d)
Control	5.78 ± 0.19^{Af}	5.68 ± 0.22^{Aj}	5.96 ± 0.20^{Aj}	-5.48 ± 0.83^{Ba}	-5.65 ± 0.24^{Ba}	-4.73 ± 0.28^{Aa}	2.36 ± 0.40^{Bg}	2.30 ± 0.17^{Bh}	3.09 ± 0.05^{Ag}	1.65 ± 0.10^{Bh}	1.76 ± 0.17^{Bi}	2.88 ± 0.07^{Ag}
1.5 % WPC	5.57 ± 0.28^{Bf}	5.92 ± 0.64^{Bi}	$6.85 \pm 0.46A^{i}$	-7.24 ± 0.59^{Bc}	-6.09 ± 0.30^{Ab}	-7.32 ± 0.20^{Bd}	2.14 ± 0.58^{Bg}	2.23 ± 0.15^{Bh}	3.29 ± 0.40^{Af}	1.74 ± 0.11^{Ag}	2.11 ± 0.17^{Ah}	2.83 ± 0.11^{Ag}
3 %WPC	11.13 ± 0.57^{Bd}	12.29 ± 0.98^{Af}	11.19 ± 0.16^{Bg}	-8.14 ± 0.56^{Cd}	-7.35 ± 0.53^{Bc}	-6.52 ± 0.20^{Ac}	3.89 ± 0.35^{Af}	3.29 ± 0.39^{Bg}	3.56 ± 0.11^{Bef}	3.25 ± 0.26^{Af}	3.42 ± 0.29^{Af}	3.12 ± 0.17^{Af}
4.5 % WPC	16.80 ± 1.30^{Bb}	18.32 ± 1.33^{Ac}	17.87 ± 0.11^{ABe}	-6.58 ± 0.50^{Ab}	-6.11 ± 0.48^{Ab}	-6.15 ± 0.18^{Ab}	8.77 ± 0.68^{Ab}	8.55 ± 0.18^{Ac}	7.58 ± 0.70^{Bd}	8.03 ± 0.84^{Ab}	7.92 ± 0.21^{Bc}	6.70 ± 0.69^{Cd}
1.5 % MRP1	8.91 ± 0.38^{Ae}	8.40 ± 0.30^{Ah}	8.20 ± 1.02^{Ah}	-8.00 ± 0.54^{Ad}	-9.02 ± 0.56^{Bd}	-7.32 ± 1.07^{Ade}	3.74 ± 0.38^{Af}	3.32 ± 0.22^{Bg}	3.68 ± 0.43^{Ae}	3.30 ± 0.37^{Af}	2.48 ± 0.06^{Bg}	3.20 ± 0.36^{Af}
3 % MRP1	13.69 ± 0.34^{Bc}	15.02 ± 0.52^{Be}	16.39 ± 0.39^{Af}	-13.23 ± 0.48^{Bg}	-15.18 ± 0.17^{Cg}	-11.19 ± 0.69^{Ag}	6.20 ± 0.31^{Cd}	6.67 ± 0.32^{Be}	7.95 ± 0.45^{Ad}	5.64 ± 0.29^{Bd}	6.33 ± 0.09^{Ae}	5.18 ± 0.30^{Ce}
4.5 % MRP1	17.13 ± 0.81^{Cb}	19.13 ± 0.73^{Ab}	18.15 ± 0.19^{Bc}	-13.18 ± 0.41^{Ag}	-19.89 ± 1.22^{Ch}	-14.06 ± 0.14^{Bi}	7.85 ± 0.35^{Bc}	9.52 ± 0.42^{Ab}	9.29 ± 0.43^{Ab}	7.42 ± 0.38^{Bc}	8.58 ± 0.20^{Ab}	8.76 ± 0.40^{Ac}
1.5 % MRP2	10.59 ± 0.34^{Bd}	10.46 ± 0.46^{Bg}	14.05 ± 1.31^{Ad}	-7.85 ± 0.90^{Acd}	-7.68 ± 0.85^{Ac}	-7.51 ± 0.11^{Ae}	4.29 ± 0.32^{Be}	3.74 ± 0.24^{Cf}	8.93 ± 0.53^{Ac}	3.70 ± 0.25^{Be}	3.40 ± 0.30^{Bf}	8.43 ± 0.67^{Ac}
3 % MRP2	17.38 ± 0.64^{Bb}	16.55 ± 1.48^{Bd}	21.04 ± 1.03^{Ab}	-9.44 ± 1.36^{Ae}	-10.61 ± 0.66^{Be}	-10.21 ± 0.46^{Bf}	7.70 ± 1.06^{Bc}	7.52 ± 0.51^{Bd}	10.40 ± 1.18^{Aa}	7.70 ± 1.01^{Bc}	7.02 ± 0.59^{Cd}	9.42 ± 0.99^{Ab}
4.5 % MRP2	27.15 ± 0.57^{Ba}	27.01 ± 0.58^{Ba}	28.18 ± 0.86^{Aa}	-11.65 ± 0.36^{Af}	-11.67 ± 0.41^{Af}	-11.96 ± 0.18^{Ah}	11.90 ± 0.09^{Ba}	10.46 ± 0.33^{Ca}	15.65 ± 0.97^{Aa}	12.17 ± 0.95^{Ba}	9.30 ± 0.56^{Ca}	13.72 ± 0.03^{Aa}

Note: (A–C)Different letters in the same line represent significant differences ($P < 0.05$). (a-j) Different letters in the same column represent significant differences ($P < 0.05$).

be related to the production technology of milk residue and protein–-protein interactions (Yang et al., 2021c).

3.3. Intrinsic fluorescence spectroscopy of MRPs

Endogenous fluorescence is commonly employed as an indicator of protein conformation (Dang et al., 2023). The λ max values of MRP1 and MRP2 both exceed 330 nm (Fig. 1D), indicating that tryptophan residues are situated within a polar environment. Fluorescence intensity (FI) of MRP1 is comparatively lower than that of MRP2, suggesting a higher degree of denaturation in MRP1 and exposure of tryptophan residues to a hydrophilic environment, leading to fluorescence quenching (Ajibola et al., 2016). This may be due to the high β-sheet content of MRP1, which makes it prone to covalent crosslinking and aggregation. As a result, tryptophan becomes trapped within protein molecules (Wu et al., 2022). MRP1 with high β-lactoglobulin causes the protein peptide chain to spread out in solution, exposing the active groups. Hence, small molecular proteins aggregate more after enhanced intermolecular interaction, leading to an increased embedding of tryptophan residues and a decrease in endogenous fluorescence intensity (Dang et al., 2023). The denaturation degree of MRP2, on the contrary, is comparatively lower and exhibits a more compact conformation, potentially attributed to its higher α-helix content and reduced β-sheet content. Wu et al. (2022) found that the protein exhibiting a high ratio of α-helix to β-sheet ratio tend to exhibit a reduced propensity for denaturation.

3.4. Flexibility and surface hydrophobicity (H_0) of MRPs

The utilization of protein hydrolase enables the elucidation of protein structural alterations and assessment of protein flexibility (Li et al., 2019). Protein flexibility is related to hydrogen bonds, van der Waals interactions, electrostatic attraction, hydrophilic interactions, covalent bonds and solubility (Mokni et al., 2015). The flexibility of MRPs was shown in Fig. 1E, with MRP2 (0.49) exhibiting higher flexibility compared to MRP1 (0.42), which was consistent with the results of solubility, surface hydrophobicity and oil holding capacity. The observed discrepancy may be attributed to the encapsulation of hydrophobic amino acid residues by protein molecules (Li et al., 2021). Additionally, MRP1 readily forms aggregates in solution (Fig. 2B), leading to an increase in molecular rigidity and a decrease in molecular flexibility, consequently resulting in diminished emulsifying properties (Fig. 3C). This phenomenon also discovered in soybean protein that exhibited a strong correlation between the emulsification ability and molecular flexibility (Li et al., 2021).

Surface hydrophobicity (H_0) is closely associated with the functional characteristics of proteins, and usually used to evaluate the exposure level of hydrophobic amino acid residues within protein (Song et al., 2021). The surface hydrophobicity of MRP2 (860.05) is significantly higher than that of MRP1 (554.25), as depicted in Fig. 1E, indicating a greater exposure of hydrophobic amino acid residues on the protein interface for MRP2. Conversely, the hydrophobic amino acid residues of MRP1 are likely to be embedded in the protein molecule, facilitating interactions between hydrophobic and covalent bonds that result in protein aggregation. Consequently, this aggregation leads to a reduction in the binding of fluorescent probes to hydrophobic groups and a decrease in the surface hydrophobicity of MRP1 (Cao et al., 2019). This study findings indicated that MRP2 has higher H_0, which exhibited superior emulsifying and foaming properties.

3.5. Turbidity, particle size and zeta potential of MRPs

Turbidity and particle size serve as indicators of protein aggregation degree (Jia et al., 2015). The particle size distribution of MRP1 and MRP2 predominantly ranges from 10 and 100 μm (Fig. 2B). The particle size of MRP2 (40 μm) is smaller than that of MRP1 (65 μm), indicating that MRP1 exhibits a propensity for aggregation, resulting in an elevation in turbidity (Fig. 2A). This observed outcome can be attributed to the reduction in protein-water interaction and the enhancement of

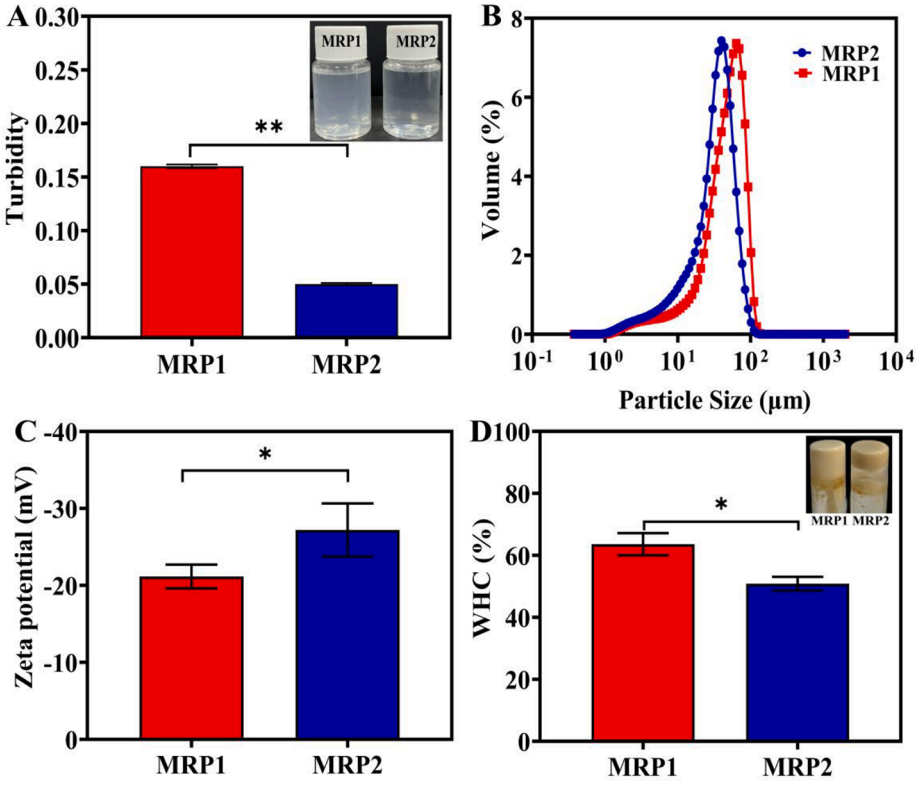

Fig. 2. (A) Turbidity of MRPs. (B) Particle size distribution of MRPs. (C) Zeta potential of MRPs. (D) Gel water holding capacity of MRPs. Symbol * show the statistical difference at $p < 0.05$.

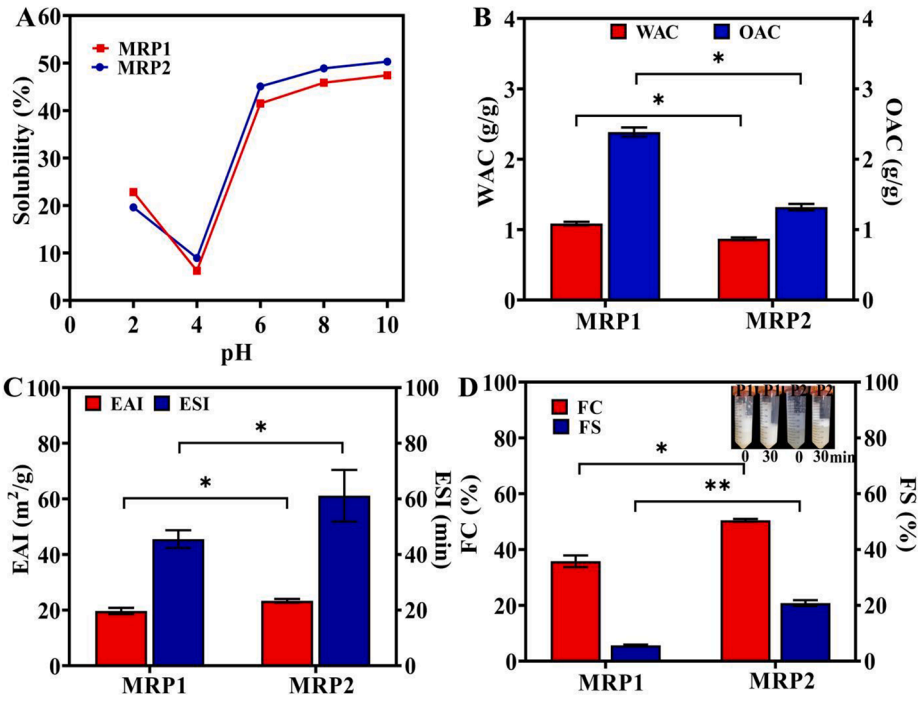

Fig. 3. (A) Solubility of MRPs. (B) WAC and OAC of MRPs. (C) EAI and ESI of MRPs. (D) FC and FS of MRPs. Symbol * show the statistical difference at $p < 0.05$.

protein–protein interaction, resulting in protein accumulation and precipitation (Cao et al., 2019). The high β-sheet content (Fig. 1C) and low negative charge distribution (Fig. 2C) of MRP1 contribute to its propensity for aggregation in solution, resulting in the formation of larger particles. Additionally, heat denaturation leads to the development of favorable gel properties (Fig. 2D). This phenomenon may be attributed to the hydrophobicity, sulfhydryl and disulfide bond interactions between whey protein and casein (Francis et al., 2019).

The zeta potential is commonly employed to quantify the extent of electrostatic interactions among protein particles (Wu et al., 2020). The Zeta potentials of MRP1 and MRP2 solutions are −21.17 mV and −27.21 mV, respectively (Fig. 2C), indicated that the surface charges of the MRP2 protein are more pronounced. The reduction in particle size of the protein solution enhances the probability of internal groups being exposed to water, resulting in an augmentation of negatively charged amino acids on the protein surface. Consequently, this enhances electrostatic repulsion between proteins (Song et al., 2021). However, the low negative charge distribution of MRP1 leads to weak electrostatic repulsion, thus promoting protein aggregation, which was consistent with the results of turbidity and particle size distribution. These above results demonstrated the excellent dispersibility and stability of MRP2.

3.6. Gelation properties of MRPs

The gel's WHC and the appearance of MRP1 and MRP2 are depicted in Fig. 2D. Notably, the WHC of MRP1 (63.61 %) was significantly higher than that of MRP2 (50.83 %). When the gel test tube is inverted, a majority of the MRP2 gel adheres to the inner wall of the test tube, while only a minor fraction of MRP1 gel exhibits this behavior. This observation suggests that MRP1 possesses superior gel properties compared to MRP2. Previous investigations have demonstrated a strong correlation between protein β-sheet content and gel formation (Zheng et al., 2021). We observed that MRP1, characterized by a higher β-sheet content, exhibited superior gel properties, thereby promoting the formation of a dense structure of yogurt (Fig. 6). Furthermore, the presence of high levels of β-lactoglobulin facilitated the formation of a stable gel network structure through disulfide bonds and electrostatic interactions (Zhang et al., 2018). This finding also elucidates the significantly enhanced strength of MRP1 gel compared to that of MRP2 gel.

3.7. Protein solubility (PS) of MRPs

The potential application value of proteins can be assessed using PS, as it is closely related to many functional characteristics of protein, including emulsification, foaming and gel properties (Sun et al., 2023). PS of MRP1 and MRP2 initially decreased and then increased with increasing pH values (Fig. 3A). At pH 4, the solubility of MRP1 (6.24 %) and MRP2 (8.93 %) reached their lowest points, indicating similar isoelectric points for both proteins. This observation aligns with the reported isoelectric point of casein by Francis et al. (2019). Within the pH range of 6 to 10, MRP2 exhibits higher solubility compared to MRP1. This observation can be attributed to the presence of a greater number of polar and hydrophobic groups on the surface of MRP2, resulting in an enhanced protein surface charge and increased bound water content, consequently leading to its improved solubility (Ma et al., 2018). However, the solubility of MRP1 is limited due to its large particle size, weak electrostatic interactions, and protein deposition in solution, thereby impeding contact between internal groups and water (Song et al., 2021).

3.8. WAC and OAC of MRPs

WAC and OAC are crucial factors in protein processing, exerting a significant influence on the sensory attributes such as taste, flavor, and texture of food products (Ma et al., 2018). WAC represents the protein matrix's ability to retain water, which is associated with protein conformation, surface charge, amino acid composition, and surface hydrophobicity (Dang et al., 2023). The WAC of MRP1 and MRP2 is 1.09 g/g and 0.87 g/g, respectively (Fig. 3B). This indicates a limited presence of soluble proteins in MRP1 and a reduced availability of polar amino acids (Ma et al., 2018). The obtained result is in accordance with the protein solubility findings (Fig. 3A). This could be attributed to the presence of a higher number of carboxyl groups and hydrated hydroxyl groups within the protein molecules, leading to a reduction in water binding sites and subsequently diminishing the interaction between proteins and water (Gao et al., 2018). Particle size and density are

influential factors that can affect the oil-holding capacity of protein powder (Gao et al., 2018). As shown in Fig. 3B, the OAC of MRP2 (2.39 g/g) was significantly higher than that of MRP1 (1.32 g/g). This showed that MRP2 hydrophobic nature and strong affinity for binding nonpolar amino acid side chains to lipids. Summary, MRP2 had excellent WAC and OAC capabilities, and is suitable for minced meat, baked dough and some sticky foods (Ma et al., 2018).

3.9. Emulsifying and foaming properties of MRPs

EAI and ESI are usually used to evaluate the emulsifying properties of protein (Dang et al., 2023). Surface net charge, solubility and surface hydrophobicity are important factors that influence the emulsifying properties of protein (Wu et al., 2020). The lower EAI and ESI values observed for MRP1 compared to MRP2 (Fig. 3C). On one hand, the exposure of more hydrophobic groups in MRP2 (Fig. 1E) facilitates its easy combination with oil. On the other hand, the reduced particle size (Fig. 2B) enhances the probability of contact between MRP2 and oil. Therefore, these results unequivocally demonstrated the exceptional emulsifying activity of MRP2. This result may be attributed to the propensity of MRP1 to aggregate in solution, resulting in the encapsulation of hydrophobic protein groups within, thereby diminishing the surface activity and adsorption capacity of protein molecules at the oil–water interface and consequently leading to a decline in MRP1 emulsifying performance. Furthermore, the diminished emulsifying performance of MRP1 can be ascribed to reduced electrostatic interactions (Fig. 2C), solubility (Fig. 3A), and surface hydrophobicity (Fig. 1E) of proteins. Stefanović et al. (2017) found that the emulsifying performance of egg white protein is highly related to solubility and hydrophobicity.

As shown in Fig. 3D, the FC of MRP1 and MRP2 are 35.82 % and 50.50 %, respectively, and the FS is 5.67 % and 20.83 %, which indicates that the FC and FS of MRP2 are higher than that of MRP1. Smaller protein particles (Fig. 2B) exhibit rapid migrate towards the air–water interface, leading to a reducing the interfacial surface tension and improving the FC ability, potentially elucidating the underlying mechanism for MRP2′s superior FC performance (Ma et al., 2018). In addition, MRP2 molecules exhibiting high H_0 levels can promote protein rearrangement at the gas–liquid interface, resulting to the formation of

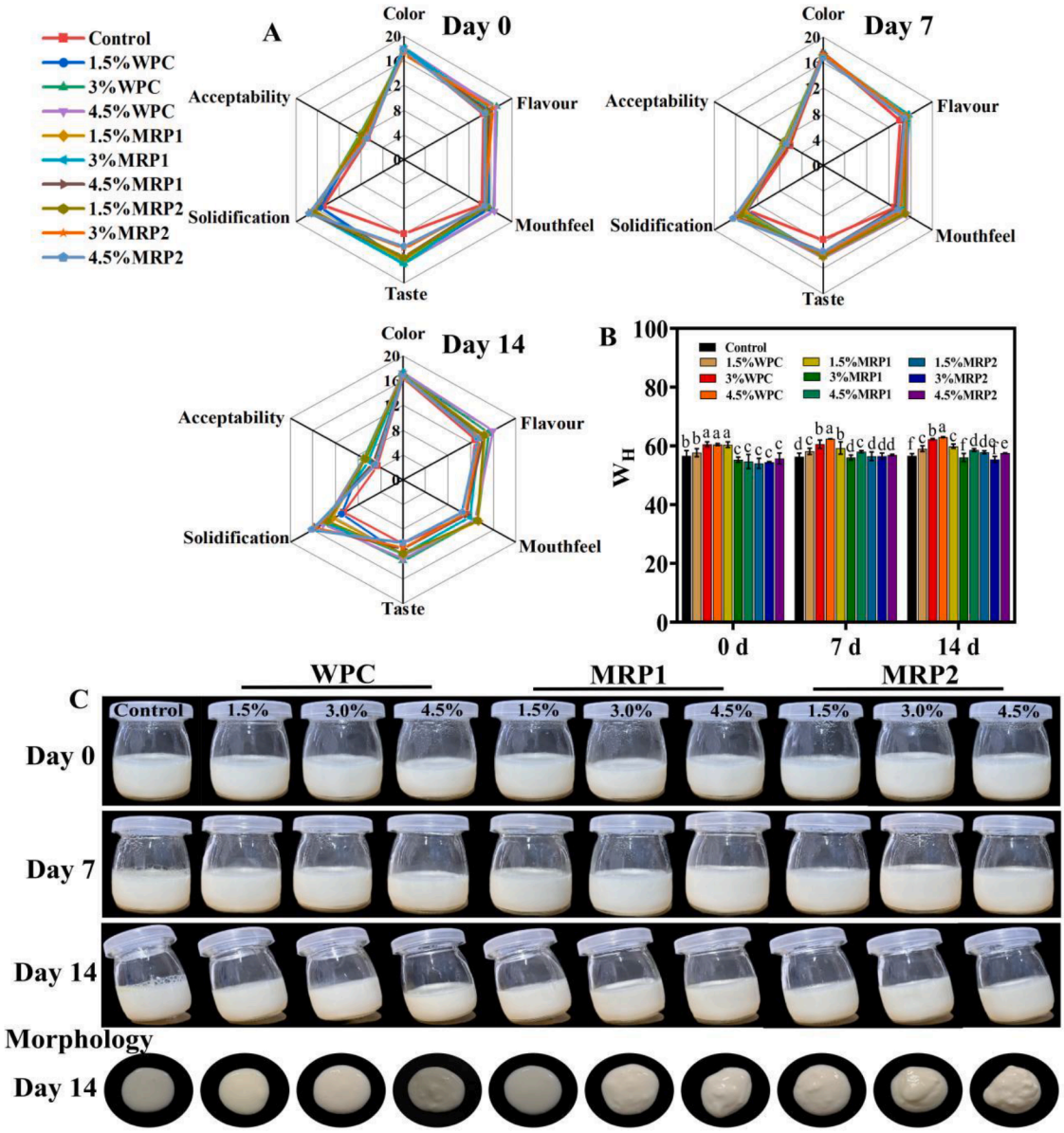

Fig. 4. Changes of sensory evaluation (A), whiteness (B) and appearance (C) of yogurt with different concentrations of MRPs and WPC stored at 4 °C for 14 days. Different letters show the statistical difference at $p < 0.05$.

viscoelastic films and subsequently enhancing FC and FS (Sun et al., 2023). Various other factors, including the protein composition, conformation, hydrophobicity and solubility, also exert an effect on the foaming characteristics of protein (Sun et al., 2023).

3.10. Sensory properties, appearance and whiteness of yogurt made from MRPs

In order to further investigate the characteristics of yogurt fortified with protein from yak milk residue, we prepared ten different types of yogurt and conducted sensory evaluations, including standard skimmed yogurt, whey protein (WPC), and two variations of milk residue protein (MRP1 and MRP2) with protein contents of 1.5 %, 3 %, and 4.5 %. The sensory scores of all yoghurts exhibited a gradual decline during the storage period (Fig. 4A). Notably, mouthfeel and taste exhibited significant changes during storage, which can be attributed to the interaction between the added protein and casein, resulting in the formation of larger granules (Fig. 4C), as well as an increase in acidity levels (Fig. 5A). Mudgil et al. (2018) observed that excessive addition of gelatin had a detrimental impact on the sensory attributes and flavor

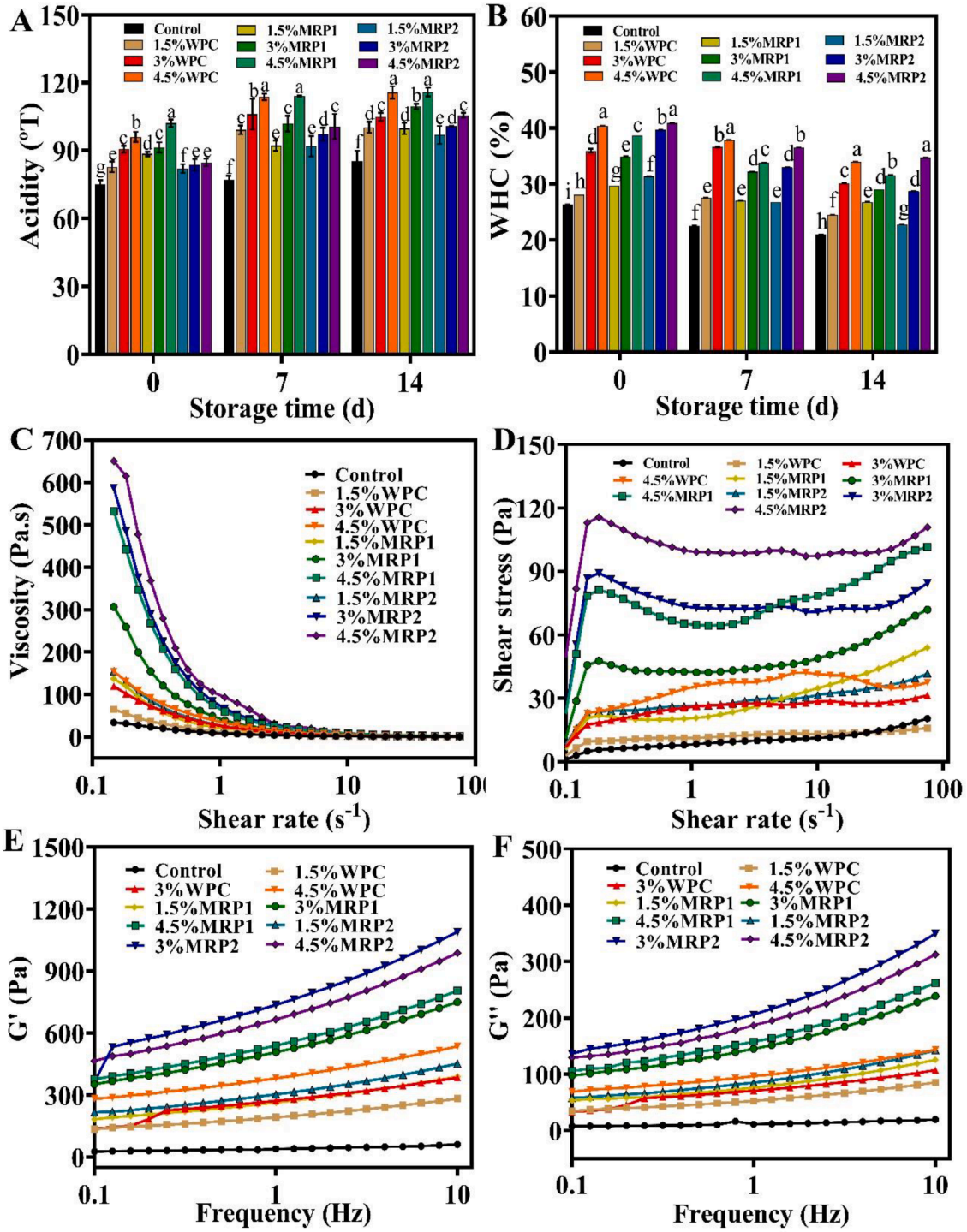

Fig. 5. Effects of different concentrations of WPC, MRP1 and MRP2 on acidity (A), water holding capacity (B), viscosity (C), shear stress (D), G' (E) and G″ (F) of skim yogurt. Different letters show the statistical difference at $p < 0.05$.

profile of camel milk yogurt. During the extended storage period, 3 % WPC yogurt (7.00) exhibited the highest score, followed by 1.5 %MRP1 yogurt (6.78) and 1.5 %MRP2 yogurt (6.67), while the control group scored the lowest at 4.56. Similar results were also found in oat protein yogurt, and excessive oat protein yogurt showed obvious bitterness (Monika et al., 2019). Furthermore, WPC and MRP1 yogurt exhibit higher whiteness levels, whereas MRP2 yogurt demonstrates lower whiteness compared to skim yogurt during the initial stages of storage (Fig. 4B). This result may be due to the disparity in amino acid composition between protein. The interaction between added protein and casein micelle alters the diffusion of incident light, thereby impeding the diffusion reaction of incident light during yogurt storage and consequently decelerating color deterioration (Yang et al., 2021b). In a word, adding appropriate amounts of MRP1 and MRP2 can improve the sensory characteristics and increase the brightness of skim yogurt.

3.11. Texture, water holding capacity (WHC), and titratable acidity (TA) of yogurt made from MRPs

To further investigate the influence of various protein additions on enhancing the stability of yogurt's physical and chemical properties, we present in Table 1 the textural characteristics of ten distinct types of yogurts. With the increase of proteins concentration (WPC, MRP1 and MRP2), there was a gradual enhancement in the hardness, gumminess, and chewiness of yogurt, while adhesiveness exhibited a gradual decrease. Notably, when the protein content reached 3 %, MRP2 yogurt demonstrated significantly higher hardness compared to WPC and MRP1 yogurts. This observation can be attributed to the interaction between MRP2 and protein in non-fat yogurt to form larger micelles. Studies have shown that the proportion of casein components (α, β and κ) and the size of casein micelle affect the gelation of yogurt and the formation of gel network (Nguyen et al., 2018). It is noteworthy that the gumminess and chewiness of MRP1 and MRP2 yogurt were significantly higher than those of WPC during the storage period. This observation indicates that MRP1 and MRP2 yogurt exhibit superior gel properties, which also accounts for their enhanced water holding capacity (Fig. 5B). These findings are consistent with the rheological characteristics observed (Fig. 5C-F). In addition, the TA content of yogurt added with MRP1 and MRP2 was significantly higher than that of the control group (Fig. 5A). However, the TA content of MRP1 and WPC yogurt remained similar during storage. This difference may be attributed to the conversion of lactose into lactic acid by probiotics, resulting in increased acidity. These findings are consistent with those reported by Xu et al. (2022) regarding hemp protein yogurt.

3.12. Rheological properties

The apparent viscosity and shear stress of 10 kinds of yogurt are shown in Fig. 5CD. It can be observed that the apparent viscosity of all yogurts exhibited a decrease with increasing shear rate, while the shear stress displayed an inverse trend. These findings indicated that all yogurts exhibited the rheological behavior of pseudoplastic fluids, displaying viscoelastic gel properties. The apparent viscosity and shear stress of yogurt are significantly influenced by the protein content. With an increase in protein content, there is a gradual rise in both the apparent viscosity and shear stress. Similar findings were observed in whey protein fortified skim yogurt (Hashim et al., 2021). The apparent viscosity and shear stress of yogurt with 3 % MRP1 and MRP2 were significantly higher than those of WPC yogurt. This may be due to the interaction between casein in milk residue protein and casein in milk to promote the formation of yogurt gel. Moreover, many other factors, such as hydrophobic interaction between protein, soluble solids and characteristics of lactic acid bacteria, will also affect the apparent viscosity of yogurt (Fuentes et al., 2020).

Storage modulus (G') and loss modulus (G″) are commonly employed to characterize the elastic and viscous properties of specimens (Du et al., 2023). The values of G' and G″ gradually increase with the increase in protein content (Fig. 5EF), indicating a continuous enhancement in the viscoelasticity of the gel. This finding aligns with the viscosity results obtained from texture analysis. Moreover, incorporation of 4.5 % MRP1 and 3 % MRP2 resulted in higher G' and G″. Yogurts with high protein addition ratio show more cross-linked particles (Fig. 4C), which may be the reason for the higher G' and G″ values of MRP1 and MRP2 yoghurts. However, yogurt with higher G' and G″ values exhibits lower mouthfeel and overall score. This phenomenon can be attributed to the high viscosity and presence of large cross-linked particles in yogurt, which significantly impact consumer perception of taste. Similar findings have also been observed in fat-free yogurt fortified with whey protein, where the addition of 50 % whey protein resulted in an increase in particle size and G' (Laiho et al., 2017).

3.13. Microstructure observation

Microstructure changes of 10 kinds of yogurt during storage are shown in Fig. 6. During storage, the structure of defatted yogurt (Control) gradually loosens, resulting in a thinner gel with larger gaps. The low-fat content in skim milk and the absence of fat globules embedded within the gel structure may contribute to a more porous yogurt structure (Gantumur et al., 2023). Compared to the control group, the incorporation of WPC, MRP1, and MRP2 into yogurt resulted in the formation of a compact gel network with well-defined pores. This phenomenon can be attributed to the covalent cross-linking between the added proteins and casein molecules, leading to the aggregation of larger protein complexes. The results further confirmed that the presence of MRP1 and MRP2 significantly enhanced the viscosity, cohesion, hardness, water holding capacity, G' and G″ of skim yogurt. Gantumur et al. (2023) demonstrated a strong correlation between the rheological properties of yogurt, such as hardness, adhesiveness, and viscosity, and the formation of protein micelles through modified whey protein and casein. However, when 4.5 % WPC was added to the yogurt along with MRP1 and MRP2, larger aggregates were formed after 7 days of storage, resulting in noticeable voids within the gel network. Excessive addition of protein may result in overfilling and phase separation of yogurt, thereby potentially compromising the integrity of the protein network structure (Wang et al., 2022). In a word, the appropriate amount of MRP can improve the network structure of yogurt.

4. Conclusions

In this study, the two types of yak milk residue proteins prepared using the alkali extraction-isoelectric precipitation method are predominantly β-folded. Specifically, MRP1 exhibits a higher degree of β-folding, β-turning, and gel properties, while MRP2 demonstrates a higher proportion of α-helix structures along with irregular curling. Additionally, MRP2 displays enhanced flexibility as well as superior emulsification, foaming ability, WAC and OAC. The non-fat yogurt, which is added with MRP2, exhibits the highest levels of hardness, gumminess, chewiness, WHC, viscosity, G', and G″. The non-fat yoghurt added with MRP1 exhibits the similar properties to the yoghurt used with commercial whey protein, the properties including sensory, texture, acidity, gel properties, and microstructure. Through comprehensive analysis, it can be concluded that the physicochemical properties of proteins derived from yak milk residue contribute to variations in its gel characteristics, wherein non-fat yogurt based on MRP1 exhibits superior quality. These findings of this study establish a solid theoretical foundation for the utilization of yak milk residue protein in the development of low and non-fat fermented dairy products.

CRediT authorship contribution statement

Guangfan Qu: Writing – original draft, Methodology, Investigation. **Feiyan Yang:** Methodology, Investigation. **Hanzhi Zhang:**

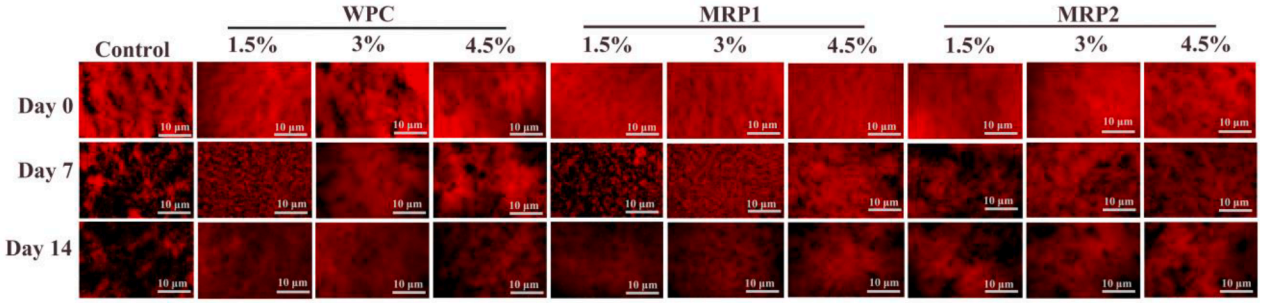

Fig. 6. Changes of microstructure of yogurt with different concentrations of WPC, MRP1 and MRP2 stored at 4 °C for 14 days.

Methodology, Investigation. **Yanfeng Liu:** Methodology, Investigation. **Xudong He:** Methodology, Investigation. **Fei Liu:** Methodology, Investigation. **Shuguo Sun:** Writing – review & editing, Project administration, Funding acquisition. **Zhang Luo:** Project administration, Funding acquisition.

Declaration of competing interest

The authors declare that they have no known competing financial interests or personal relationships that could have appeared to influence the work reported in this paper.

Data availability

Data will be made available on request.

Acknowledgments

The project was financially supported by Central Committee of Tibet Autonomous Region guides the Special Project of Local Science and Technology Development (XZ202202YD0004C); Major Project of Changsha Science and Technology Program (kh2301028). The funders declare no role in the study design, data collection and analysis, preparation of the manuscript or decision to publish.

References

Ajibola, C. F., Malomo, S. A., Fagbemi, T. N., & Aluko, R. E. (2016). Polypeptide composition and functional properties of African yam bean seed (Sphenostylis stenocarpa) albumin, globulin and protein concentrate. *Food Hydrocolloids, 56*, 189–200. https://doi.org/10.1016/j.foodhyd.2015.12.013

Atallah, A. A., Morsy, O. M., & Gemiel, D. G. (2020). Characterization of functional low-fat yogurt enriched with whey protein concentrate, Ca-caseinate and spirulina. *International Journal of Food Properties, 23*(1), 1678–1691. https://doi.org/10.1080/10942912.2020.1823409

Anema, S. G. (2021). Heat-induced changes in caseins and casein micelles, including interactions with denatured whey proteins. *International Dairy Journal, 122*, Article 105136. https://doi.org/10.1016/j.idairyj.2021.105136

Ban, Q., Liu, Z., Yu, C., Sun, X., Jiang, Y., Cheng, J., & Guo, M. (2020). Physiochemical, rheological, microstructural, and antioxidant properties of yogurt using monk fruit extract as a sweetener. *Journal of Dairy Science, 103*(11), 10006–10014. https://doi.org/10.3168/jds.2020-18703

Cao, H., Jiao, X., Fan, D., Huang, J., Zhao, J., Yan, B., Zhou, W., Zhang, W., Ye, W., & Zhang, H. (2019). Catalytic effect of transglutaminase mediated by myofibrillar protein crosslinking under microwave irradiation. *Food Chemistry, 284*, 45–52. https://doi.org/10.1016/j.foodchem.2019.01.09

Chen, L., Chen, N., He, Q., Sun, Q., Gao, M. R., & Zeng, W. C. (2022). Effects of different phenolic compounds on the interfacial behaviour of casein and the action mechanism. *Food Research International, 162*, Article 112110. https://doi.org/10.1016/j.foodres.2022.112110

Ding, Y. X., Gao, Y. H., Sun, J. X., Li, C. Q., Yue, X. Q., & Shao, J. H. (2022). Influence of ultrasonic treatment on functional properties and structure of tussah pupa protein isolate. *Journal of Insects as Food and Feed, 8*(10), 1133–1148. https://doi.org/10.3920/jiff2021.0116

Dang, Y., Ren, J., Guo, Y., Yang, Q., Liang, J., Li, R., Zhang, R., Yang, P., Gao, X., & Du, S. K. (2023). Structural, functional properties of protein and characteristics of tofu from small-seeded soybeans grown in the Loess Plateau of China. *Food Chemistry: X, 18*, Article 100689. https://doi.org/10.1016/j.fochx.2023.100689

Du, H. X., Wang, X. P., Yang, H. G., Zhu, F., Cheng, J. R., Peng, X. X., Lin, Y. H., & Liu, X. M. (2023). Effects of mulberry pomace polysaccharide addition before fermentation on quality characteristics of yogurt. *Food Control, 153*, Article 109900. https://doi.org/10.1016/j.foodcont.2023.109900

Dai, S., Corke, H., & Shah, N. P. (2016). Utilization of konjac glucomannan as a fat replacer in low-fat and skimmed yogurt. *Journal of Dairy Science, 7063–7074*. https://doi.org/10.3168/jds.2016-11131

Francis, M. J., Glover, Z. J., Yu, Q., Povey, M. J., & Holmes, M. J. (2019). Acoustic characterisation of ph-dependant reversible micellar casein aggregation. *Colloids and Surfaces A: Physicochemical and Engineering Aspects, 568*, 259–265. https://doi.org/10.1016/j.colsurfa.2019.02.026

Fuentes, J., Ferńandez, I., Ferńandez, H., Śanchez, J., Aleḿan, R., & Navarro-Alarcon, M. (2020). Quantification of bioactive molecules, minerals and bromatological analysis in carao (Cassia grandis). *Journal of Agricultural Science, 12*, 88–94. https://doi.org/10.5539/jas.v12n3p88

Gantumur, M. A., Sukhbaatar, N., Jiang, Q. W., Enkhtuya, E., Hu, J. L., Gao, C. Z., Jiang, Z. M., & Li, A. L. (2023). Effect of modified fermented whey protein fortification on the functional, physical, microstructural, and sensory properties of low-fat yogurt. *Food Control, 155*, Article 110032. https://doi.org/10.1016/j.foodcont.2023.110032

Gao, L. L., Li, Y. Q., Wang, Z. S., Sun, G. J., & Qi, X. M. (2018). Physicochemical characteristics and functionality of tree peony (Paeonia suffruticosa Andr.) seed protein. *Food Chemistry, 240*, 980–988. https://doi.org/10.1016/j.foodchem.2017.07.124

Hashim, M. A., Nadtochii, L. A., Muradova, M. B., Proskura, A. V., Alsaleem, K. A., & Hammam, A. R. A. (2021). Non-fat yogurt fortified with whey protein isolate: Physicochemical, rheological, and microstructural properties. *Foods, 10*(8), 1762. https://doi.org/10.3390/foods10081762

Jia, D., You, J., Hu, Y., Liu, R., & Xiong, S. (2015). Effect of $CaCl_2$ on denaturation and aggregation of silver carp myosin during setting. *Food Chemistry, 185*, 212–218. https://doi.org/10.1016/j.foodchem.2015.03.130

Li, R., Wang, X., Liu, J., Cui, Q., Wang, X., Chen, S., & Jiang, L. (2019). Relationship between molecular flexibility and emulsifying properties of soy protein isolate-glucose conjugates. *Journal of Agricultural and Food Chemistry, 67*(14), 4089–4097. https://doi.org/10.1021/acs.jafc.8b06713

Li, H., Li, F., Wu, X., & Wu, W. (2021). Effect of rice bran rancidity on the emulsion stability of rice bran protein and structural characteristics of interface protein. *Food Hydrocolloids, 121*, Article 107006. https://doi.org/10.1016/j.foodhyd.2021.107006

Lee, H. S., Song, M. W., Kim, K. T., Hong, W. S., & Paik, H. D. (2021). Antioxidant effect and sensory evaluation of yogurt supplemented with hydroponic ginseng root extract. *Foods (Basel, Switzerland), 10*(3), 639. https://doi.org/10.3390/foods10030639

Lee, I., & Kang, T. Y. (2024). Heat-moisture-treated rice starches with different amylose and moisture contents as stabilizers for nonfat yogurt. *Food Chemistry, 436*, Article 137746. https://doi.org/10.1016/j.foodchem.2023.137746

Laiho, S., Williams, R. P. W., Poelman, A., Appelqvist, I., & Logan, A. (2017). Effect of whey protein phase volume on the tribology, rheology and sensory properties of fat-free stirred yoghurts. *Food Hydrocolloids, 67*, 166–177. https://doi.org/10.1016/j.foodhyd.2017.01.017

Mudgil, P., Jumah, B., Ahmad, M., Hamed, F., & Maqsood, S. (2018). Rheological, micro-structural and sensorial properties of camel milk yogurtas influenced by gelatin. *LWT-Food Science and Technology, 98*, 646–653. https://doi.org/10.1016/j.lwt.2018.09.008

Monika, B. G., Albina, B., & Stephan, D. (2019). Enrichment of yoghurt with oat protein fractions: Structure formation, textural properties and sensory evaluation. *Food Hydrocolloids, 86*, 146–153. https://doi.org/10.1016/j.foodhyd.2018.03.019

Ma, M., Ren, Y., Xie, W., Zhou, D., Tang, S., Kuang, M., & Du, S. K. (2018). Physicochemical and functional properties of protein isolate obtained from cottonseed meal. *Food Chemistry, 240*, 856–862. https://doi.org/10.1016/j.foodchem.2017.08.030

Mokni, G. A., Maklouf, G. I., Sila, A., Blecker, C., Danthine, S., Attia, H., Bougatef, A., & Besbes, S. (2015). Effects of enzymatic hydrolysis on conformational and functional properties of chickpea protein isolate. *Food Chemistry, 187*, 322–330. https://doi.org/10.1016/j.foodchem.2015.04.109

Nguyen, H. T. H., Afsar, S., & Day, L. (2018). Differences in the microstructure and rheological properties of low-fat yoghurts from goat, sheep and cow milk. *Food*

Research International, 108, 423–429. https://doi.org/10.1016/j.foodres.2018.03.040

Qin, D. D., Yang, F. Y., Hu, Z. M., Liu, J. L., Wu, Q., Luo, Y., Yang, L. F., Han, S. A., & Luo, F. J. (2021). Peptide T8 isolated from yak milk residue ameliorates H_2O_2-induced oxidative stress through Nrf2 signaling pathway in huvec cells. *Food Bioscience, 44*, Article 101408. https://doi.org/10.1016/j.fbio.2021.101408

Sun, H., Sun, J. L., Dou, N. X., Li, J. Z., Hussain, M. A., Ma, J. G., Hou, J., & C.. (2023). Characterization and comparison of structure, thermal and functional characteristics of various commercial pea proteins. *Food Bioscience, 53*, Article 102740. https://doi.org/10.1016/j.fbio.2023.102740

Song, B., Zhang, Y., Yang, B., Zhu, P., Pang, X., Xie, N., Zhang, S., & Lv, J. (2021). Effect of different temperature-controlled ultrasound on the physical and functional properties of micellar casein concentrate. *Foods (Basel, Switzerland), 10*(11), 2673. https://doi.org/10.3390/foods10112673

Stefanović, A. B., Jovanović, J. R., Dojčinović, M. B., Lević, S. M., Nedović, V. A., Bugarski, B. M., & Knežević-Jugović, Z. D. (2017). Effect of the controlled high-intensity ultrasound on improving functionality and structural changes of egg white proteins. *Food and Bioprocess Technology, 10*(7), 1224–1239. https://doi.org/10.1007/s11947-017-1884-5

Silva, M., Zisu, B., & Chandrapala, J. (2018). Influence of low-frequency ultrasound on the physico-chemical and structural characteristics of milk systems with varying casein to whey protein ratios. *Ultrasonics Sonochemistry, 49*, 268–276. https://doi.org/10.1016/j.ultsonch.2018.08.015

Wu, Y. Y., Xiang, X. L., Liu, L., An, F. P., Geng, F., Huang, Q., & Wei, S. F. (2022). Ultrasound-assisted succinylation comprehensively improved functional properties of egg white protein. *LWT - Food Science and Technology, 171*, Article 114155. https://doi.org/10.1016/j.lwt.2022.114155

Wu, W., Li, F., & Wu, X. (2020). Effects of rice bran rancidity on oxidation, structural characteristics and interfacial properties of rice bran globulin. *Food Hydrocolloids, 110*, Article 106123. https://doi.org/10.1016/j.foodhyd.2020.106123

Wang, J., Liu, B. Y., Qi, Y., Wu, D., Liu, X. T., Liu, C. L., Gao, Y. W., Shi, J. H., Fang, L., & Min, W. H. (2022). Impact of Auricularia cornea var. Li polysaccharides on the physicochemical, textual, flavor, and antioxidant properties of set yogurt. *International Journal of Biological Macromolecules, 206*, 148–158. https://doi.org/10.1016/j.ijbiomac.2022.02.141

Xu, J. X., Xu, X. Y., Yuan, Z. H., Hua, D., Yan, Y. X., Bai, M., & Song, H. (2022). Effect of hemp protein on the physicochemical properties and flavor components of plant-based yogurt. *LWT-Food Science and Technology, 172*, Article 114145. https://doi.org/10.1016/j.lwt.2022.114145

Yang, F. Y., He, X. D., Chen, T., Liu, J. L., Luo, Z., Sun, S. G., Qin, D. D., Huang, W., Tang, Y. P., Liu, C. A., & Luo, F. J. (2021a). Peptides isolated from yak milk residue exert antioxidant effects through Nrf2 signal pathway. *Oxidative Medicine and Cellular Longevity, 2021*, 9426314. https://doi.org/10.1155/2021/9426314

Yang, M., Li, N. N., Tong, L. T., Fan, B., Wang, L. L., Wang, F. Z., & Liu, L. N. (2021b). Comparison of physicochemical properties and volatile flavor compounds of pea protein and mung bean protein-based yogurt. *LWT-Food Science and Technology, 1522*, Article 112390. https://doi.org/10.1016/j.lwt.2021.112390

Yang, F. F., Luo, Z., Xie, S. W., Liu, C. A., Huang, W. Y, & Sun, S. G. (2021c). Study on nutrition, flavor characteristics and antioxidant activity of yak milk residue at different elevations in Tibet. *Science and Technology of Food Industry, 42*(11), 81–88. https://doi.org/10.13386/j.issn1002-0306.2020090265

Zheng, L., Wang, Z. J., Kong, Y., Ma, Z. L., Wu, C. L., Regenstein, J. M., Teng, F., & Li, Y. (2021). Different commercial soy protein isolates and the characteristics of Chiba tofu. *Food Hydrocolloids, 110*, Article 106115. https://doi.org/10.1016/j.foodhyd.2020.106115

Zhang, Q., Wang, C., Li, B., Li, L., Lin, D., Chen, H., & Yang, W. (2018). Research progress in tofu processing: From raw materials to processing conditions. *Critical Reviews in Food Science and Nutrition, 58*(9), 1448–1467. https://doi.org/10.1080/10408398.2016.1263823